3D Numerical Study of Crystal Rotation Effect on Three-Phase Line in Floating Zone Silicon

Han, Xue-Feng
Research Institute for Applied Mechanics, Kyushu University

Liu, Xin
Research Institute for Applied Mechanics, Kyushu University

Nakano, Satoshi
Research Institute for Applied Mechanics, Kyushu University

Harada, Hirofumi
Research Institute for Applied Mechanics, Kyushu University

他

https://doi.org/10.15017/2740961

出版情報：九州大学応用力学研究所所報. 157, pp.7-11, 2020-03. Research Institute for Applied Mechanics, Kyushu University
バージョン：
権利関係：

3D Numerical Study of Crystal Rotation Effect on Three-Phase Line in Floating Zone Silicon

Xue-Feng HAN [*1], Xin LIU[*1], Satoshi NAKANO[*1],
Hirofumi HARADA[*1], Yoshiji MIYAMURA[*1] and Koichi KAKIMOTO[*1]
E-mail of corresponding author: *han0459@riam.kyushu-u.ac.jp*

(Received January 28, 2020)

Abstract

In this paper, we have developed a model for a 200 mm floating zone silicon crystal growth process to investigate solid–liquid interface. To study the effect of high-frequency (HF) electromagnetic (EM) heating on the solid-liquid interface shape, HF-EM and heat transfer calculations were conducted in three dimensions. By considering 3D Marangoni and EM forces at the free surface, a more accurate interface shape has been obtained. the results showed that local growth rate became more inhomogeneous when the rotation speed of the crystal was increased. However, a more homogeneous three-phase line could be obtained with a high rotational crystal speed.

Keywords: *Computer simulation, Floating zone technique, Semiconducting silicon*

1. Introduction

Floating zone (FZ) silicon is used in high-voltage power devices with its low impurity levels [1]. One of the challenges in competing with Czochralski (CZ) silicon lies in increasing the diameter of the crystal. For CZ silicon, crystals with a 300 mm diameter are already being produced commercially and studied [2]. The limitations of increasing the diameter of FZ silicon crystal are mainly because relatively high electrical power increases the possibility of arcing in the region of the electromagnetic (EM) current supplies [3]. The solidification front easily breaks out in the radial direction. To solve the arcing problem, H. J. Rost et al. [4] suggested using low frequency (1.7 MHz) to grow FZ crystals. For the breaking out problem, it is believed that deflection of the three-phase line causes melt spillage. R. Menzel calculated the current density along the three-phase line, indicating that the current density becomes more inhomogeneous with increasing crystal diameter [5]. High power density below the current supplies causes deflection of the three-phase line and the breaking out problem.

To analyze the complex flow and three-dimensional phenomena, a three-dimensional numerical model is required. There are numerous previous studies on the simulation of 100 mm FZ silicon crystal growth [6-10]. A. Sabanskis et al. [6] have modeled the doping process from the gas in FZ process and compared the calculation result with the experimental data. The influence of cooling gas also has been discussed through axis-symmetric global simulation [7]. G. Ratnieks et al. calculated phase boundaries, temperature distribution, and dopant concentration for 100 mm FZ silicon [8, 10, 11]. The melt flow caused by EM force and Marangoni force have been discussed in three dimensions. G. Ratnieks [11] also proposed a 2D axis-symmetric simulation model of 200 mm FZ silicon to investigate the phase boundary and compare it with experimental result.

However, there has been no reported numerical study of three-dimensional 200 mm FZ silicon to investigate the deflection of the three-phase line. The deflection could hinder further increases in FZ silicon crystal diameter. Therefore, in the present study, we proposed a three-dimensional 200 mm FZ model to analyze the deflection of the three-phase line.

2. Numerical models

Fig. 1 shows the EM model for calculation of the EM field in the FZ process. The dimensions of the feed rod, crystal, and inductor coil are referred to in previous

*1 Research Institute for Applied Mechanics, Kyushu Univ.

research [11]. The diameter of the feed rod is 150 mm. The diameter of the crystal is 200 mm. There are three side slits and one main slit in the induction coil. The induction heating is operated at a high frequency of around 3 MHz. Induction heating and EM force are neglected in the domain deeper than skin depth. Skin depth is 0.26 mm in the silicon melt when the working frequency is 3 MHz. Compared to the calculation domain of silicon of several hundred millimeters, the skin depth is considered the boundary of the calculation domain. The impedance boundary condition is used to model the skin depth effect.

The simulation domain is the space between the crystal and the furnace. The boundary of the model is the

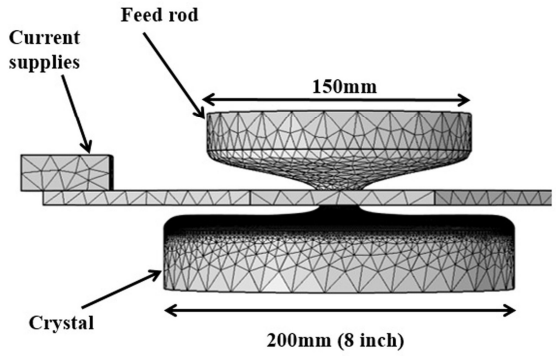

Fig.1 3D numerical model for high-frequency EM field in the FZ growth system.

surface of the crystal, melt and inductor. The magnetic and electric fields are expressed in terms of the magnetic vector potential $\boldsymbol{A}$ and the electric scalar potential V. The governing equation to solve the time-harmonic equation can be written as:

$$\boldsymbol{\nabla} \times (\mu_0^{-1} \boldsymbol{\nabla} \times \boldsymbol{A}) + \sigma \boldsymbol{\nabla} V + j\omega\sigma \boldsymbol{A} = \boldsymbol{J_e} \qquad (1)$$

where σ is electrical conductivity, μ_0 is the permeability, j is an imaginary unit, ω is the angular frequency, and $\boldsymbol{J_e}$ is the externally generated current density. The calculation for 3D EM field is conducted by the AC/DC simulation module in the commercial software COMSOL.

Heat transfer and fluid flow calculations are conducted using open-source library OpenFOAM 2.3.1. Fig. 2 shows the calculation model for heat transfer and fluid flow. The phase boundary of silicon is assumed to be fixed. The free surface of the melt and melting front are obtained from the previous study of 200 mm FZ silicon [11]. The free surface and melting front are assumed to be axis-symmetric.

The crystallization interface is calculated. The shape of the crystallization interface is coupled with the

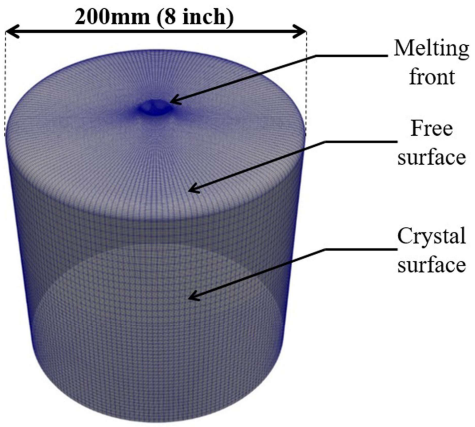

Fig.2 3D model for heat transfer calculation. The melt and crystal are included in the same calculation domain. The diameter of the crystal is 200 mm. The model consists of structured mesh.

temperature field. The rotation of the crystal is considered. The heat transfer calculation was conducted using the finite volume method. The governing equations in the steady-state melt flow are the continuity equation (Eq. (2)) and the Navier–Stokes equation (Eq. (3)):

$$\boldsymbol{\nabla} \cdot (\rho \boldsymbol{U}) = 0 \qquad (2)$$

$$\boldsymbol{\nabla} \cdot (\rho \boldsymbol{U}\boldsymbol{U}) = \boldsymbol{\nabla} \cdot (\mu \boldsymbol{\nabla} \boldsymbol{U}) - \boldsymbol{\nabla} p + \rho g \qquad (3)$$

where ρ is the melt density, $\boldsymbol{U}$ is the velocity vector in the melt, μ is the viscosity of the melt, p is the pressure, and g is the gravitational acceleration constant. The heat transfer in the melt and crystal is solved by the following equation:

$$\rho \boldsymbol{U} \boldsymbol{\nabla} h = \boldsymbol{\nabla} \cdot (a \boldsymbol{\nabla} h) \qquad (4)$$

where h is enthalpy and a is thermal diffusivity.

3. Results

During the FZ process, direct heating from the induction coil leads to a high temperature at the free surface of the silicon melt. This technique causes a high gradient of temperature and electromagnetic flux density. The Marangoni and EM forces at the free surface contribute to melt flow at the free surface, which was reported in the previous study [12]. Fig. 3a shows the calculated current density distribution at the free surface. Below the tips of the three side slits, the current density is higher. Below the main slit, the current density is lower. In the vicinity of the current supplies, the current density is higher.

By using the current density distribution at the free surface, the heating power at the free surface was calculated. Accordingly, the temperature and flow field

were calculated. Fig. 3b shows the temperature distribution at the free surface. Below the tip of the side slits, the temperature is high because of the high power density. Below the main slit, the temperature is low because of the low power density. The temperature field is not symmetric, which is affected by the flow and the rotation of crystal. The maximum temperature difference is 70 K in the melt. The temperature difference is higher than previous 2D calculation [10] because the maximum temperature of the 2D model is an averaged value along the azimuthal direction.

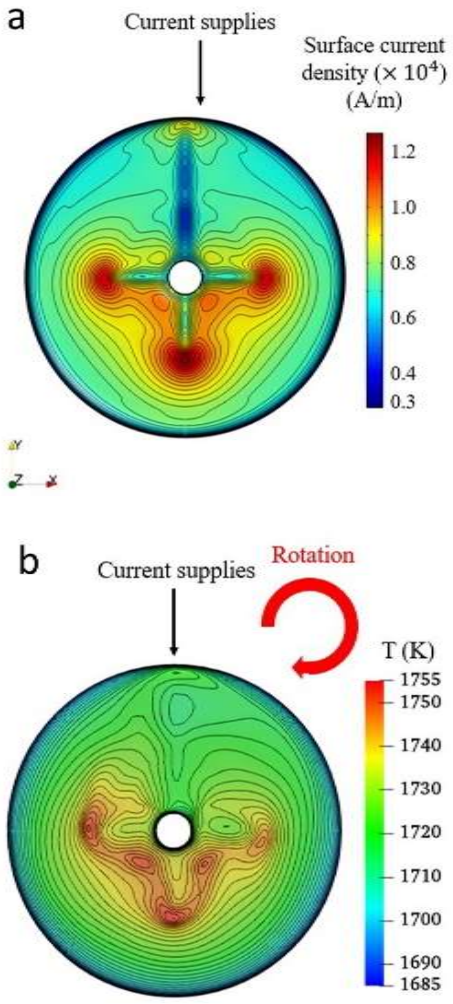

Fig.3 a. Surface current density distribution at the free surface of the melt. b. Temperature distribution at the free surface of melt.

The shape of the crystallization interface is crucial in FZ silicon crystal growth. Particularly, the periphery of the interface (three-phase line between gas, crystal, and melt) should be stable during growth. Deflection of the three-phase line leads to a lateral growth of crystal.

In Fig. 4, the local growth rate fluctuation is

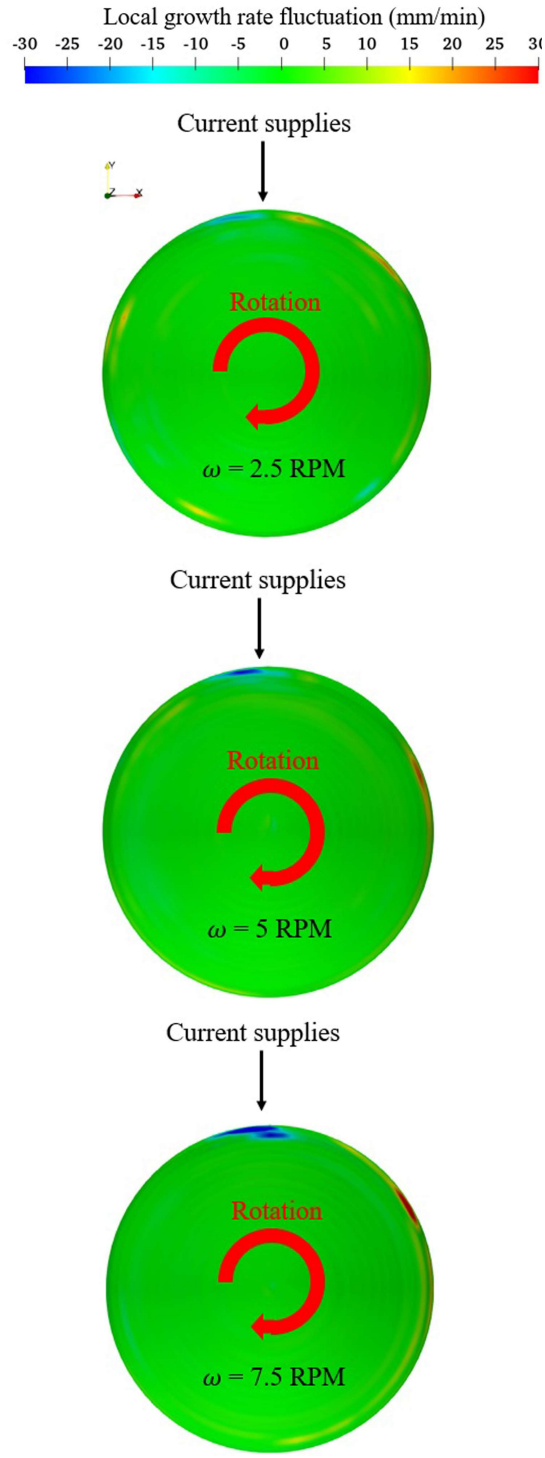

Fig.4 Local growth rate fluctuation at the crystallization interface under crystal rotational speeds of 2.5 RPM, 5 RPM, and 7.5 RPM.

calculated at the interface under different rotational crystal speeds. The local growth rate fluctuation depends on the rotation speeds of the crystal and azimuthal interface deflection. The pulling rate is the same at

different rotational speeds of the crystal. Different rotational speeds affect the shape of the interface. The variation in local growth rate occurs at the periphery of the interface because of the inhomogeneous EM heating at the three-phase line. Particularly, in the vicinity of the current supplies, a significant negative growth rate occurs. The negative growth rate means that the crystal could melt locally and instantly. When the rotational speed of the crystal is increased, the interface becomes more homogeneous. And the variation in the local growth rate becomes larger.

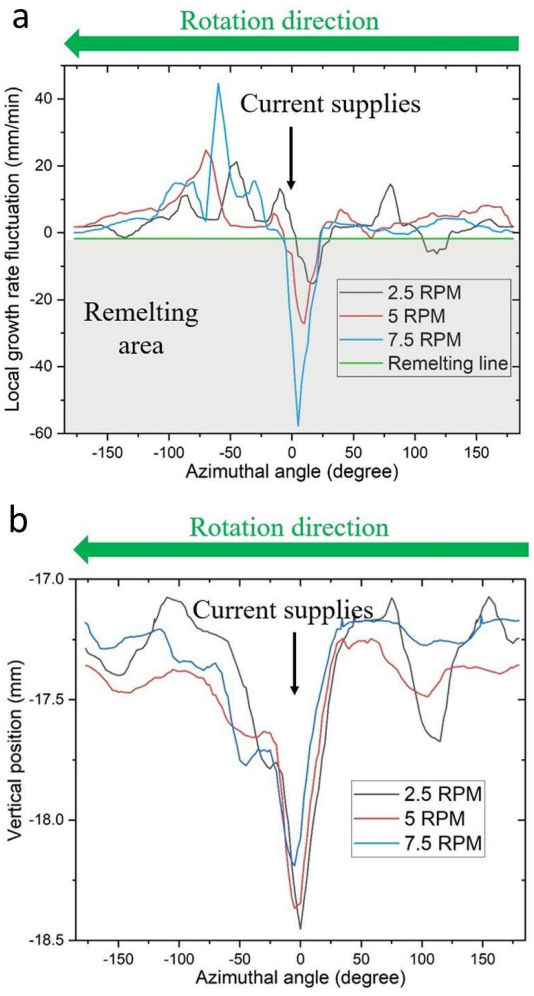

Fig.5 a. Comparison of the local growth rate fluctuation along the three-phase line among different crystal rotational speeds. The temporal re-melting area is indicated in the shade. b. Comparison of the positions of the three-phase line among different crystal rotational speeds.

Fig. 5a shows the local growth rate fluctuation at the three-phase line along the azimuthal direction. Below the current supplies, the local growth rate fluctuation is negative in different crystal rotational speeds. In the cases of 2.5 RPM, 5 RPM, and 7.5 RPM, the minimum local growth rate fluctuations were approximately −18 mm/min, −28 mm/min, and −57 mm/min, respectively. This means that the temporal re-melting phenomenon is more significant at high crystal rotational speeds. Moreover, the maximum local growth rate fluctuation also increased when the rotational speed of the crystal increased.

Fig. 5b shows the vertical positions of the three-phase lines at different crystal rotational speeds. The deviation of the vertical position of the three-phase line is < 1.5 mm. In the case of 2.5 RPM, the three-phase line has the lowest position below the current supplies because of strong EM heating under the current supplies. The position of the three-phase line is not homogeneous because EM heating is not homogeneous at the three-phase line. When the speed of the crystal is increased to 5 RPM, the lowest position becomes higher and the three-phase line becomes more homogeneous. The deviation of the vertical position of the three-phase line is decreased to 1 mm when the rotational speed of the crystal is increased to 7.5 RPM. Though the re-melting phenomenon becomes more significant when the rotational speed of the crystal is increased, the duration of the temporal re-melting region is shorter. Therefore, a high rotational crystal speed could improve the homogeneity of the three-phase line.

4. Conclusion

In this paper, a high-frequency EM model and heat transfer model for a 200 mm FZ process are constructed. The FZ model presented in the paper considered the three-dimensional Marangoni force, EM force, and interface deflection. The local growth rate is also taken into account according to the deflection of interface and rotation speeds. The deflection of the three-phase line is obtained at different rotational speeds of the crystal. The deflection below the current supplies was found to be most significant. The downward deflection has the potential risk of melt spillage from the crystal or lateral growth to break the symmetry of the crystal. At higher crystal rotational speeds, the local growth rate increases in fluctuation. However, the duration of the fluctuating local growth rate is shorter at higher crystal rotational speeds. Therefore, at higher crystal rotational speeds, the three-phase line is more homogenous, and the risk of melt spillage or lateral growth is reduced.

Acknowledgment

This work was partly supported by the New Energy

and Industrial Technology Development Organization (NEDO) under Ministry of Economy, Trade and Industry.

References

1) W. Zulehner, Historical overview of silicon crystal pulling development, Materials Science and Engineering: B, 73,7-15, 2000
2) R. Yokoyama, T. Nakamura, W. Sugimura, T. Ono, T. Fujiwara, K. Kakimoto, Time-dependent behavior of melt flow in the industrial scale silicon Czochralski growth with a transverse magnetic field, Journal of Crystal Growth, 519, 77-83, 2019
3) L. Altmannshofer, M. Grundner, J. Virbulis, Silicon single crystal produced by crucible-free float zone pulling, in, US Patents, 2005.
4) H.J. Rost, R. Menzel, A. Luedge, H. Riemann, Float-Zone silicon crystal growth at reduced RF frequencies, Journal of Crystal Growth, 360, 43-46, 2012
5) R. Menzel, Growth Conditions for Large Diameter FZ Si Single Crystals, PhD thesis, 2013
6) Sabanskis, K. Surovovs, J. Virbulis, 3D modeling of doping from the atmosphere in floating zone silicon crystal growth, Journal of Crystal Growth, 457, 65-71, 2017
7) Sabanskis, J. Virbulis, Simulation of the influence of gas flow on melt convection and phase boundaries in FZ silicon single crystal growth, Journal of Crystal Growth, 417, 51-57, 2015
8) G. Ratnieks, A. Muiznieks, L. Buligins, G. Raming, A. Mühlbauer, A. Lüdge, H. Riemann, Influence of the three dimensionality of the HF electromagnetic field on resistivity variations in Si single crystals during FZ growth, Journal of crystal growth, 216, 204-219, 2000
9) Mühlbauer, A. Muiznieks, J. Virbulis, A. Lüdge, H. Riemann, Interface shape, heat transfer and fluid flow in the floating zone growth of large silicon crystals with the needle-eye technique, Journal of crystal growth, 151, 66-79, 1995
10) G. Ratnieks, A. Muižnieks, A. Mühlbauer, G. Raming, Numerical 3D study of FZ growth: dependence on growth parameters and melt instability, Journal of crystal growth, 230, 48-56, 2001
11) G. Ratnieks, Modelling of the Floating Zone Growth of Silicon Single Crystals with Diameter up to 8 Inch, PhD thesis, 2007
12) G. Raming, A. Muižnieks, A. Mühlbauer, Numerical investigation of the influence of EM-fields on fluid motion and resistivity distribution during floating-zone growth of large silicon single crystals, Journal of crystal growth, 230, 108-117, 2001